בס"ד

Ben-Gurion University of the Negev

Department of Physics

Ph.D. Research Proposal

Development of Compact Detector Systems, Utilizing Raman and Broadband Coherent Anti-Stokes Raman Scattering Spectroscopies

By Itamar Malka

Supervisor: Prof. I. Bar

March 2012

Supervisor:

Chairman of Ph.D. studies committee:

תקציר

זיהוי חומרי נפץ ומרכיבים שונים היכולים לשמש ליצירת חומרי נפץ תוצרת בית הינה בעיה כלל עולמית, אשר למרות המאמצים הרבים המושקעים בפתרונה, נותרה עדיין ללא מענה הולם. מטרת המחקר המוצע הינה זיהוי חומרים ושאריות של חומרים אלו ע"י חישה מקרוב ומרחוק. לשם כך נפתח וניישם מערכות מודולריות וקומפקטיות המתבססות על ספקטרוסקופיית ראמן ספונטני ועל שיטה שתפותח כאן לראשונה, ספקטרוסקופיית coherent anti-Stokes Raman scattering (CARS) רחבת סרט בפיזור אחורי (B-CARS) ע"י פולסים באורך תת ננו-שניה. ספקטרוסקופיות אלו יאפשרו כושר גילוי גבוה ועירור בו זמני של אופני התנודה הויברציונים בתחום ספקטרלי נרחב. קבלת החתימות הספקטרליות של דוגמאות שונות תאפשר דגימה בזמני מדידה קצרים יחסית והקטנת התרעות השווא. אנו מצפים כי מערכות מודולריות ופשוטות אלו יוכלו בעזרת מערכת של ספריית נתונים לשמש לזיהוי ולמיפוי חומרי נפץ וחומרים אחרים במצבים שונים.

התוצאות הראשוניות שהתקבלו ממדידות שנעשו בעזרת ספקטרומטר ראמן, שפותח על ידינו, המבוסס על ציין לייזר ירוק בעוצמה נמוכה מראות יכולת גלוי גבוהה של נוזלים ושל חלקיקים של חומרים שונים, בזמני מדידה של מספר שניות. בגלל המיקוד החזק על הדוגמא מערכת זו מאפשרת מדידת ספקטרומי רמאן אפילו מחלקיקים בודדים שהמסה שלהם היא כ-150 ng. מערכת זו תהווה בסיס לבנית מערכות רמאן ו-B-CARS רחב סרט, מאחר והמרכיבים העיקריים במערכות זהים, מלבד המסננים והלייזר המעורר, שיוחלף בלייזר שבב זעיר (מיקרוצ'יפ) Nd:YAG. ההרמוניה השניה של לייזר זה תשמש לעירור רמאן ספונטני, או B–CARS, כך שבתהליך האחרון חלק מקרן ההרמוניה השניה יספק את קרן השאיבה והחלק הנותר יועבר דרך סיב פוטוני לקבלת קרן סטוקס רחבת הסרט. מערכות אלו יאפשרו קבלת ספקטרא אופיניים, מיפוי של חלקיקים המצויים על משטחים שונים, בחינת הרגישויות השונות ובייחוד בחינת השיפור המושג בגלוי ע"י מערכת ה-B-CARS הפולסי, לעומת מערכות הרמאן הספונטני.

Introduction

The knowledge of the contents of specific samples or the identification of particular molecules in a sample can be of great value in different applications, including homeland security[1,2] and forensic science.[3,4,5,6] The need to detect and locate hidden explosives, land mines,[7] as well as the availability of conventional military explosives, duo to regime changes, and the accessible information on the internet regarding methods for producing improvised explosive devices (IEDs), have made the detection of traces of explosives or related compounds even more important than before.[8]

Some of the most commonly investigated methods use laser spectroscopies,[1,4,8,9,10,11,12,13,14,15,16,17] considered to be capable to selectively identify species of interest and expected to have the highest potential for reaching necessary sensitivity levels and desired ranges. Indeed, different methods were developed for detection of explosives vapors. [12,13,18,19,20] However, detection of explosives in the gas phase can become extremely difficult, since most of them are characterized by low vapor pressures and may even be found in unconfined volumes where their original vapor might be dispersed by normal airflow, resulting in poor sensitivity and false alarms.[1,2,9]

Nevertheless, explosives are known to be “sticky” and could be readily adsorbed upon surfaces, so that a single monolayer of a typical nitro-explosive corresponds to a surface density of about 3×10^{14} molecules/cm^2 (~ 100 ng/cm^2).[21] Therefore, high chances of finding particulate explosive around nonhermetically sealed explosives or due to contamination of the explosives containers or nearby objects, exist. These reasons have motivated research toward development of methods for remote or standoff detection and identification of bulk or trace quantities of explosives or other compounds in the condensed phase.[6,22,23,24]

One approach that can be considered for detection is that based on vibrational spectroscopies,[25] including Raman and infrared, which are based on inelastic scattering and absorption, respectively. In these spectroscopies, the vibrational frequencies, related to vibrational modes of molecules, allow exposing the signatures related to molecular structures. The advantage of these methods is that they provide quite detailed information on the examined samples. In particular, this characteristic of Raman spectroscopy, together with the requirement of only minimal sample preparation, point to its potential for real-time detection of harmful compounds.

Indeed, spontaneous Raman scattering,[8,10,11,26,27] and its nonlinear variant, coherent anti-Stokes Raman scattering (CARS)[28,29] have been developed for trace amounts of liquid and solid organic and inorganic samples at ranges up to hundreds of meters. Although standoff detection is required in many scenarios, it should be pointed out, that the methods for sensing presence of explosive devices at large distances have to overcome different difficulties, including eye-safety for the beam used for excitation, free beam and signal paths, absorption and scattering losses in air (wavelength-dependent), the signal intensity decrease inversely with the distance squared and the complicated and high cost systems that not always could be foreseen to be appropriate for field measurements. It is worth pointing out, that at least under some scenarios, *point detection* and identification of explosives is required and would be of interest. To test this option, we will use Raman scattering and CARS spectroscopies for developing novel compact spectrometers, and therefore their principles are shortly described here.

a) Spontaneous Raman scattering

Spontaneous Raman scattering[30,31] is one of the processes a molecule can undergo, while interacting with light. This inelastic process involves conversion of one photon to another, so that a laser "pump" beam at a frequency, ω_p, illuminates the sample, and due to inelastic scattering a signal is generated at the Stokes and anti-Stokes frequencies, ω_S and ω_{AS}, respectively (the latter signal being much weaker) (Fig. 1). The spontaneous Raman intensity scattered into 4π steradians is given by:[32]

$$I_{Raman} = 4\pi\sigma_R L N I_p \quad , \qquad (1)$$

where σ_R is the Raman scattering cross section, L is the sample length, N is the molecular density and I_p is the focused beam intensity at the corresponding optical frequency. The cross sections for Raman scattering, σ_R, are typically of 10^{-30} cm^2 sr^{-1}, leading to intensities of the scattered light of the order 10^{-7} of that of the incident light. Therefore, and due to possible florescence interference, spontaneous Raman signal is hard to detect, resulting in complexity and development of highly expensive systems.

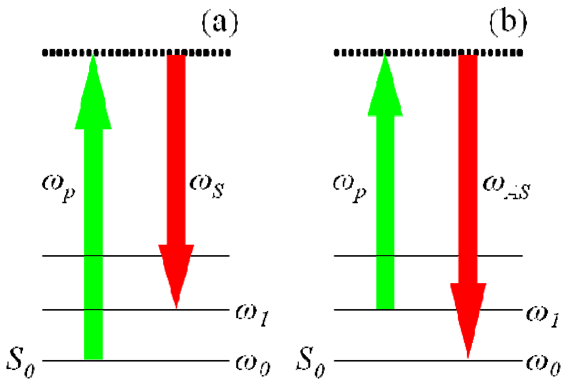

Fig. 1. Energy level diagram for spontaneous Raman, (a) Stokes scattering, where ω_p is the pump frequency and ω_S the Stokes frequency, (b) anti-Stokes scattering, where ω_p is the pump frequency and ω_{AS} is the anti-Stokes frequency.

b) *Coherent anti-Stokes Raman scattering*

To achieve higher sensitivities, one can replace spontaneous Raman with two- or four-wave parametric processes as stimulated Raman scattering (SRS) and CARS.[30,31] These nonlinear scattering processes provide unique spectroscopic tools, promising high molecular specificity and detailed structural information, based on the Raman signatures.

Specifically, CARS is a coherent four-wave mixing process, involving the third order dielectric susceptibility, $\chi^{(3)}_{CARS}$, arising from the third-order polarization:[33]

$$P^{(3)}(\omega_{AS}) = \chi^{(3)}_{CARS} E_p(\omega_P)^2 E_S(\omega_S) \quad , \quad (2)$$

where $E_p(\omega_P)$ and $E_S(\omega_S)$ are the electric fields of the pump and Stokes beams, respectively. In the CARS process, a particular Raman transition is coherently driven by the incident ω_p and ω_S laser beams, and subsequently the vibrational coherence is probed by a third laser beam (usually ω_p), giving rise to the (anti-Stokes) CARS signal designated as ω_{CARS} (Fig. 2). Due to its nonlinear nature, CARS benefits from the characteristics of multiphoton processes and significant signal enhancement over spontaneous Raman.

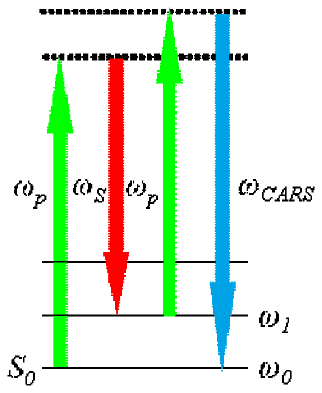

Fig. 2. Energy level diagram for CARS, where ω_p is the pump frequency, ω_S the Stokes frequency, the probe frequency, ω_{pr}, which usually is similar to ω_p, and $\omega_{CARS} = 2\omega_p - \omega_S$ is the CARS frequency.

One can estimate the CARS to spontaneous Raman signal ratio by expressing the maximum resonance CARS signal, I_{CARS}^{MAX}, in terms of σ_R, as:[34]

$$I_{CARS}^{MAX} = \left(\frac{16\pi^2 c^2}{\omega_{as}^3 n^2 h\Gamma} NL\sigma_R\right)^2 I_p^2 I_s \qquad , \qquad (3)$$

where N is the molecular density, 2Γ is the linewidth of the vibrational resonance, n is refractive index at ω_{as}, and I_p and I_S are the focused beam intensities at the corresponding optical frequencies. The ratio between the CARS and the Raman signal for a given species depends of course on the values of the parameters of Eqs. (1) and (3), and, as shown in Refs. 31 and 32, is typically of several orders of magnitude.

Due to these benefits there has been extensive use of CARS in spectroscopic studies and in a variety of applications, including the use for detecting bacterial endospores,[35] imaging of cells[33,36,37] and standoff detection of various species.[28,38] Very recently, narrowband ns excitation was employed in our group for obtaining the back-reflected CARS, i.e., backward CARS (B-CARS)[32,39] signal in order to detect solid particles of explosives and explosive related compounds. It was shown that the positions of the dominant spectral features of spontaneous Raman of each compound remain essentially the same in B-CARS, but the latter allows much higher detection sensitivity. The CARS detection method to be developed in the present proposal relies on B-CARS. However, in attempt to overcome an inherent drawback of the narrowband B-CARS method, namely, the need to scan the Stokes frequency, in this project we will utilize and develop a broadband B-CARS system, based on sub-ns pulses, for obtaining the spectral signatures of a variety of compounds.

Objectives

The main objectives of this project are to develop, optimize and test novel methods and technologies for unprecedented, highly sensitive point and standoff detection of a broad variety of hazardous materials or their mixtures in condensed phases. This will be accompanied by characterization of the structural and spectroscopic features of the materials. The systems to be developed are a low cost compact modular Raman spectrometer, based on a green laser pointer and a relatively simple Raman or broadband sub-ns B-CARS spectrometer, based on a Nd:YAG microchip laser. These systems will be used for detection and imaging of traces of compounds in real time. The pulsed Raman and broadband CARS systems are expected to reduce the signal acquisition times and the latter also to overcome an inherent drawback of the narrowband B-CARS method, namely, the need to scan the Stokes frequency. This will be the first attempt to explore the application of the novel method of visible, sub-ns ultra-broadband multiplex CARS for point and standoff detection, benefiting from simultaneous excitation of the vibrational modes in the entire vibrational range and enabling capturing the spectra in even shorter time and with improved intensity.

Real time detection and identification of explosives and related compounds is a major issue in efforts to develop defense against terrorism and might be of importance also for inspection in the battlefield. The envisaged setups are expected to be relatively simple and robust devices, applicable for deployment in security checkpoints of sensitive installations. Moreover, it is anticipated that these systems will find their use for monitoring the Raman and CARS spectra of other species as well as for imaging of their appearance.

Methodology

As mentioned above, this study will be devoted to Raman and broadband sub-ns B-CARS detection of explosives, in attempt to find the best conditions for their rapid detection. For Raman excitation, a single beam is required, while for the broadband CARS, two laser beams at ω_p and ω_S coincide on the sample. In CARS, a particular Raman transition is coherently driven by the ω_p and ω_S incident laser beams, and subsequently the vibrational coherence is probed by a third laser beam (usually ω_p), giving rise to the CARS signal. Since the ω_S beam will be broadband in our experiment, as shown in Fig. 3, it will allow excitation of all the vibrational states in a specific sample, depending on the Raman cross sections, and therefore capturing of the signal in the entire vibrational range of the fundamentals.

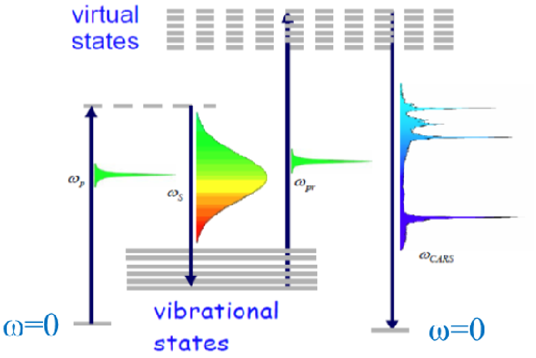

Fig. 3. Schematics of the concept for broadband CARS, where ω_p is the pump frequency, ω_S marks the span of broadband Stokes frequencies, the probe frequency will be similar to ω_p in our experiment, and $\omega_{CARS} = 2\omega_p - \omega_S$ are the CARS frequencies of the detected vibrational states.

The setups for the spontaneous Raman and B-CARS spectrometers (Fig. 4) include several similar main components, but differ in the exciting sources. The sources for these spectrometers include the frequency doubled green laser pointer (Laser Pointer, 30 mW) and a *Q*-switched Nd:YAG microchip laser (Horous Laser). A short description on the Raman system will be given in the section of preliminary results, while here the broadband CARS system will be described.

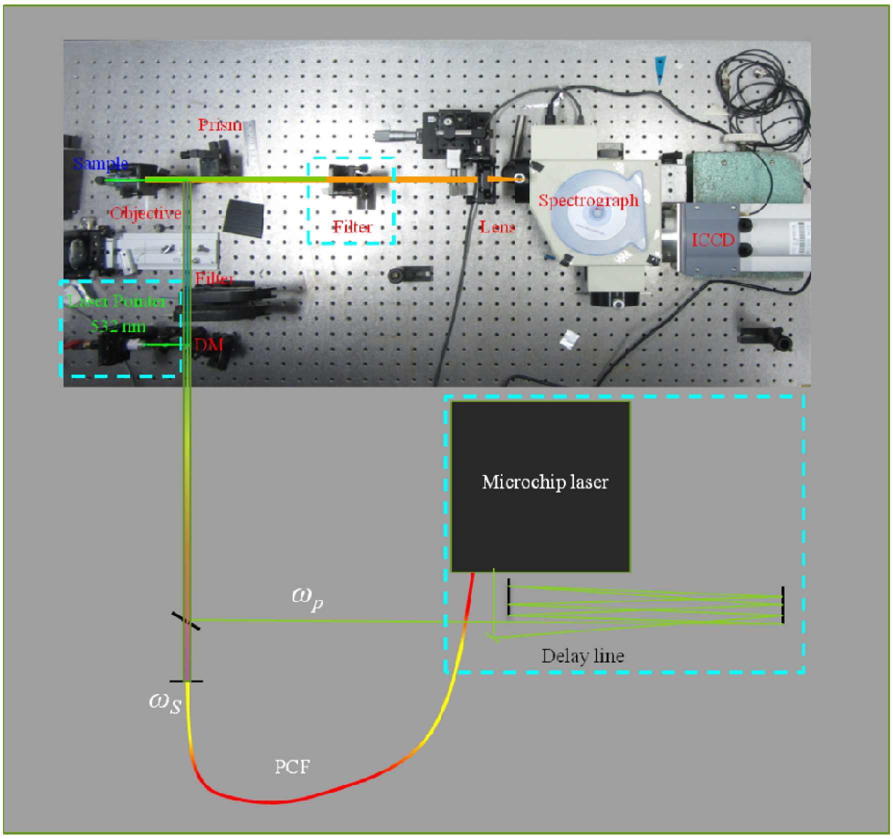

Fig. 4. The experimental setup, including the marked components and an intensified charge-coupled device (ICCD) and dichroic mirror (DM). The components surrounded by the dashed lines have to be changed in the different systems.

In principle, the passively Q-switched[40] microchip laser[41,42] consists of a sub-millimeter piece of solid-state (Nd:YAG) gain material, polished flat and parallel on two sides to create a cavity (the cavity mirrors are dielectrically deposited directly onto the polished surface) which is excited by a diode laser. The frequency doubled output of this laser will be split in two portions, where one of them after amplification, will be used as the pump and the other will be coupled into a photonic crystal fiber (PCF) to generate the supercontinuum (SC), [43,44] which will serve as the ω_S beam. The SC beam covers the 480 – 1700 nm range and therefore by delivering it through long and short wavepass edge filters the required Stokes beam in the 535 – 660 nm range will be obtained. The pump and Stokes beams will be spatially and temporally (by adjusting the delay line of the ω_p beam in Fig. 4) overlapped and combined by a dichroic filter (Semrock, FF520-Di02), before focusing them onto the sample to induce the simultaneous vibrational coherences in the ultrabroad frequency range. The detection of the broadband B-CARS signal will be performed similarly to that of the Raman signal (see below), except that the long wavepass edge filter will be replaced by a short wavepass edge filter (Semrock, SP01-532RU).

Upon blocking the PCF output, the spontaneous Raman signal will also be measured, allowing direct comparison of the sensitivity of the same system for Raman and CARS detection. The sub-ns operation of the microchip laser will provide high peak intensity and therefore enhanced Raman signal, compared to that obtained with the continuous laser pointer (see below). Also, since it operates in a pulsed mode, it will enable detection of the signal with the intensified charge coupled device (ICCD) operated in gated mode, reducing the noise signal from the background and therefore resulting in higher signal to noise ratios (SNR).

A rough estimate of the ratio of the broadband B-CARS signal to that obtained in the spontaneous Raman can be obtained while considering the foreseen experimental conditions and using Eqs. (1) and (3). This ratio for the characteristic ~1050 $\mathrm{cm^{-1}}$ Raman active vibration of KNO_3 where, $N \sim 1.2x10^{28}$ $1/\mathrm{m}^3$, $n \sim 1.5$, $\sigma_R \sim 5x10^{-30}$ $\mathrm{cm^2/sr}$ and the optical parameters as $\Gamma \sim 5$ $\mathrm{cm^{-1}}$, $\omega_p \sim 18796$ $\mathrm{cm^{-1}}$, $I_P = 1.5x10^{14}$ $\mathrm{W/m^2}$, $\omega_S \sim 16666$ $\mathrm{cm^{-1}}$, $I_S = 7.5x10^7$ $\mathrm{W/m^2}$ and $L \sim 0.5$ mm for the sample length, is calculated as 10^7 (for a biconvex focusing lens of 5 cm diameter and 17.5 cm focal length). Since the detected B-CARS signal, is estimated to be only about 4 % of the forward CARS, [45] the ratio of CARS to spontaneous Raman signal is reduced to about five orders of magnitude, implying much higher detection sensitivity for the former. This enhancement is particularly important, as the intensity decreases inversely with the distance squared:[32]

$$I \propto n = n_0 \frac{D^2}{16}\frac{1}{r^2} \qquad , \qquad (4)$$

where n is the number of photons reaching the detector, n_0 is the total number of the generated photons and D is the collecting lens diameter. Under the above mentioned conditions and with a collecting lens of D = 5 cm, the estimated distance for signal detection can be obtained from Eq. (4). It turns out that the B-CARS signal can be detected at a distance of ten meters (SNR ~ 3), showing the possible promise of the broadband B-CARS system for both *point and standoff detection*.

As mentioned above the system will serve for measuring the Raman and CARS spectra of the different compounds, but also for mapping traces of a particular compound, or mixtures of compounds on different substrates. The mapping will be attained by positioning the sample on an *x,y* translational stage and scanning it in ~ 1 μm steps. An application on the LabView software will be developed for driving the translational stage and for monitoring the spectra from the different positions by the ICCD. Successive recordings of the spectra from the different positions will allow computation of two-dimensional (2D) Raman maps, based on characteristic Raman shifts of measured sample.

Preliminary results

In some scenarios, point detection of explosive residues, suspect shipments and screening of hidden explosives carried by travelers on airlines is required. Under such circumstances the people, vehicles, and packages can be checked repeatedly, if necessary, leading to their permitted or forbidden entrance to a particular section. Therefore, we constructed and tested the performance of the Raman spectrometer, which allows monitoring liquids solids and even single solid particles from residues of latent human fingerprints at short acquisition times and high SNRs (> 100). Since the overall system is modular, compact and can be readily made portable, it can be easily applied to detection of harmful compounds and particularly to explosive residues on latent fingerprints.

Up today, our efforts were focused on detection of different compounds by Raman spectroscopy with the newly developed compact modular Raman spectrometer (Fig. 4). As has been mentioned, the experimental setup for the spontaneous Raman spectrometer is very similar to that of the B-CARS experiment and consists of a commercial low-power frequency doubled green laser pointer at 532 nm (Laser Pointer) operating by a DC power supply for prolonged operation time and stability with < 30 mW power. The laser beam was turned by a dichroic mirror (DM) and a right angle tiny prism (3 mm) and tightly focused through the x40/0.65 microscope objective to provide a power of 10 mW on the samples. The backscattered Raman signal was collimated by the same objective and following blocking of the laser beam by a long wavepass edge filter (Semrock, LP03-532RE) it was focused onto a pinhole (100 µm) located in front of the slit spectrometer and eventually reaching the air cooled 1024 x 1024 ICCD, driven by the Solis 4.15 software.

Following optimization of the alignment of the laser beam and the collection optics in the newly constructed Raman spectrometer, the spectra of different samples were measured. In order to confirm the operation of the newly constructed Raman spectrometer we present the measured Raman spectra of 2-phenylethyl alcohol (liquid), as measured by a commercial system, i.e., a micro-Raman spectrometer (LabRam UV HR, Jobin-Yvon, with excitation wavelength of ~ 785 nm and 10 mW power) and with our compact system as presented in Fig. 5, panels (a) and (b), respectively. It is immediately seen that the spectra resemble very much, although the spectral resolution in the compact system is somewhat poorer due to limited resolution of the spectrometer and the higher linewidth of the exciting laser. In addition, the spectrum measured by the compact spectrometer benefits from a better SNR in the high frequency range, due to better performance of the ICCD in the high frequency range. It is obvious that the structured and characteristic spectral signature, in the entire spectral range, provides the means for the identification of the measured compound.

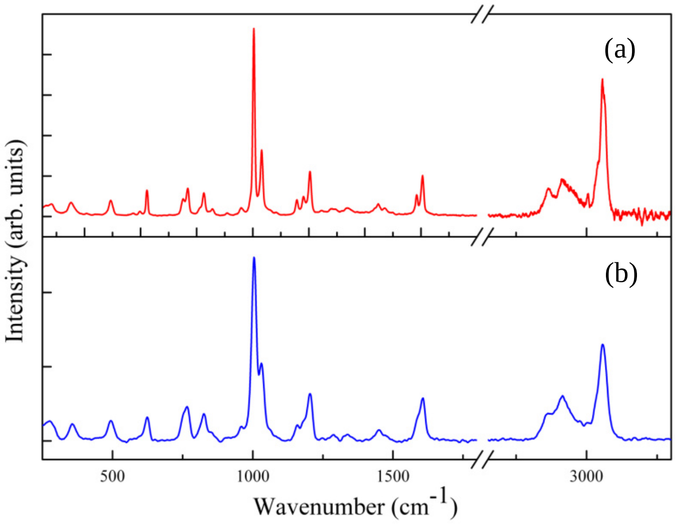

Fig. 5. Raman spectra of 2-phenylethyl alcohol measured by a commercial confocal Raman microscope (a) and by the newly constructed Raman spectrometer (b).

The new system was also used for measurement of Raman spectra of liquids (Fig. 6) and solid samples (Fig. 7). The liquid samples, including hydrogen peroxide (a), acetone (b), which are precursors for synthesis of triacetone triperoxide (TATP), methanol (c) and isopropanol (d), were hold in 2 cm diameter glass vials, while the solid samples were prepared by applying small amounts of dispersed powder on glass microscopic slides, which were attached to a stand on a *x,y* motorized 1" translation stage (Thorlabs, Z8250) and positioned in front of the objective. The spectra were measured while operating the ICCD in the continuous mode for integration times of 10-15 s. To obtain the full spectral range, each spectrum was scanned across the ICCD by moving the grating two times. The resulting signals were transferred to a computer where they were processed and displayed. Figures 6 and 7 clearly show that each of the compounds has a unique Raman signature. It is interesting to note that even the spectral signatures of two dinitrotoulene isomers, i.e, 2,4 dinitrotoluene and 3,4 dinitrotoluene, shown in panels (e) and (f) of Fig. 7, respectively, differ; meaning that the signatures allow to unravel even very delicate

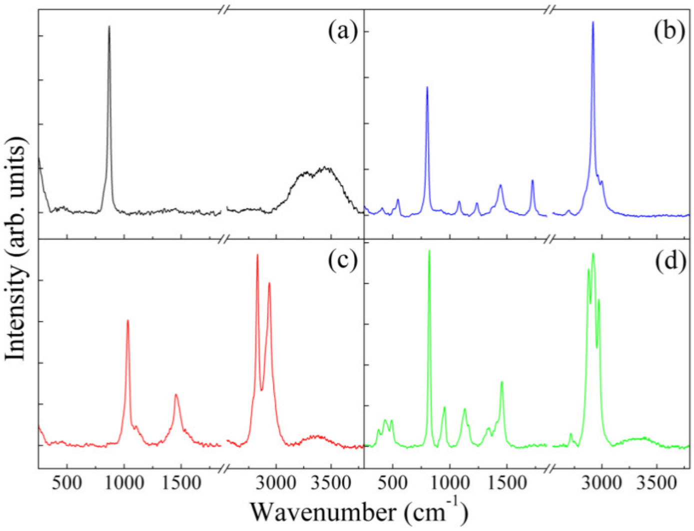

Fig. 6. Raman vibrational spectra of several liquid samples, including hydrogen peroxide (a), acetone (b), methanol (c) and isopropanol (d), measured with the compact Raman spectrometer.

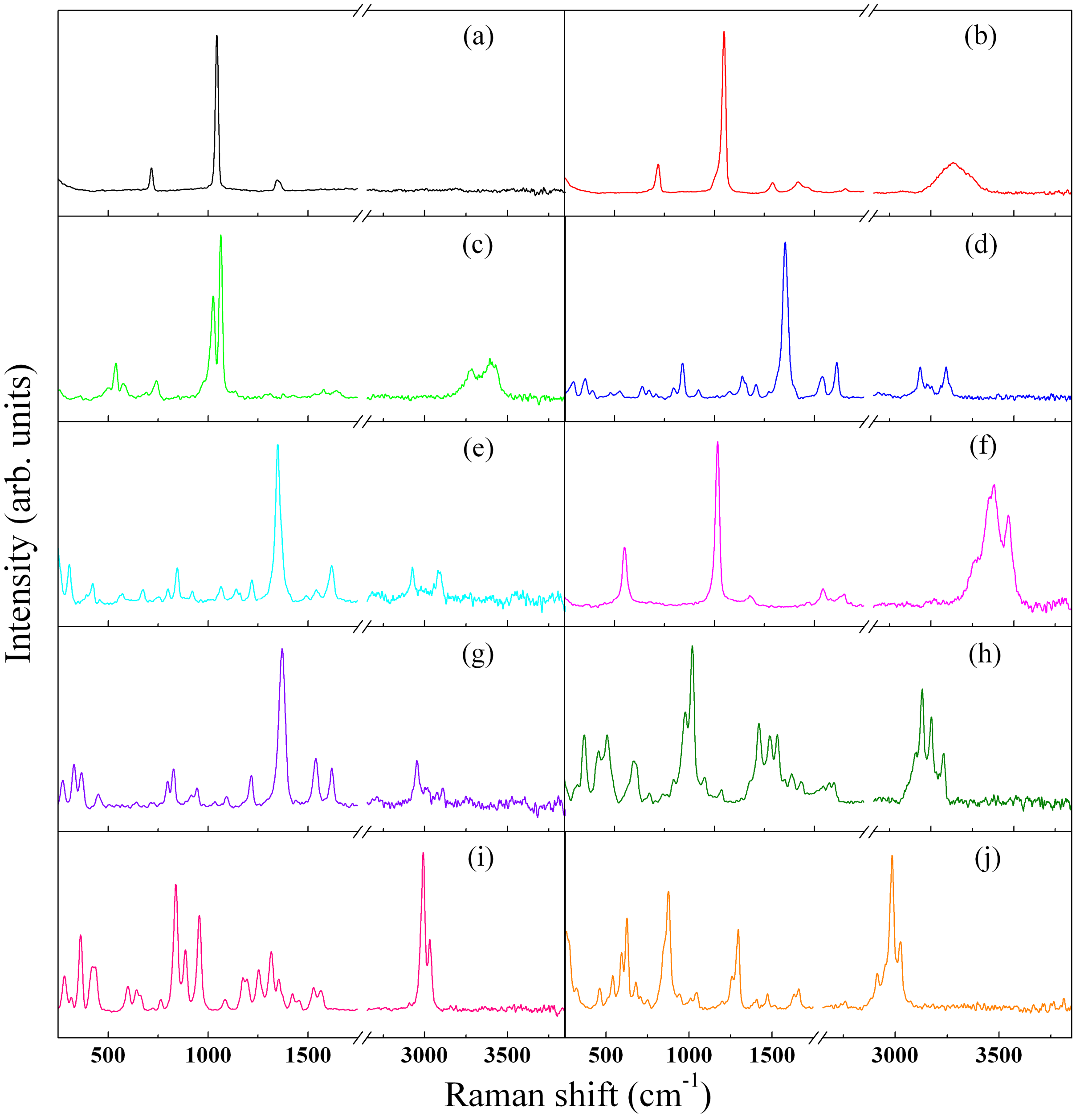

Fig. 7. Raman vibrational spectra of several solid samples, including (a) potassium nitrate, (b) ammonium nitrate, (c) urea nitrate, (d) urea, (e) 2,4 dinitrotoluene, (f) 3,4 dinitrotoluene, (g) 2,4,6-trinitrotoluene, (h) RDX, (i) HMX and (j) PTEN, measured with the compact Raman spectrometer.

changes in the structure. In particular, if these signatures would be compared to the spectra in a database, it would be possible to identify a sample with the compound with which it had the highest correlation.

Considering that the exciting laser is tightly focused, the possibility of detecting individual particles by this system was tested. For measuring those extrinsic compounds that were left within a fingerprint, samples were prepared as follows. The hands of a volunteer were cleaned with ordinary soap, rinsed in water and dried and aged in air. Then the index finger was stained by touching the powder of a particular compound, spread on a clean glass slide. Excessive powder was rubbed off by hitting the contaminated hand with a glove, till powder was unobservable on the finger by the naked eye. Finally, this finger was pressed onto a clean microscopic slide, which was located in front of the objective. The Raman spectrometer was used to first locate the position of a particular particle by first photographing the region of the fingerprint and then scanning the sample in the *x,y* directions (2 μm steps), till a specific particle chosen for measurement was found to strongly "blink". This point was selected as the measurement point for obtaining the Raman spectrum. As can be seen from Figs. 8(a) – (c), spectral signatures of potassium nitrate, urea nitrate and 2,4 dinitrotoluene, respectively, were obtained. The spectra match very well those presented in Fig. 7 for these compounds, clearly showing that the pattern differs from one particle to the other. Also shown, in the right part of the figure, are micrographs of the individual particles of the different compounds, used for measuring the spectra. The residues of the recently handheld materials cannot be distinguished by their morphology, however, their Raman spectral signature can differentiate between them, even if particles as small as 20 μm with estimated mass of 150 ng were analyzed. Once again, it is expected that these particles could be easily identified by comparing the measured spectra to

Raman spectra appearing in a data base, providing the possibility to detect them even when only a single particle is present.

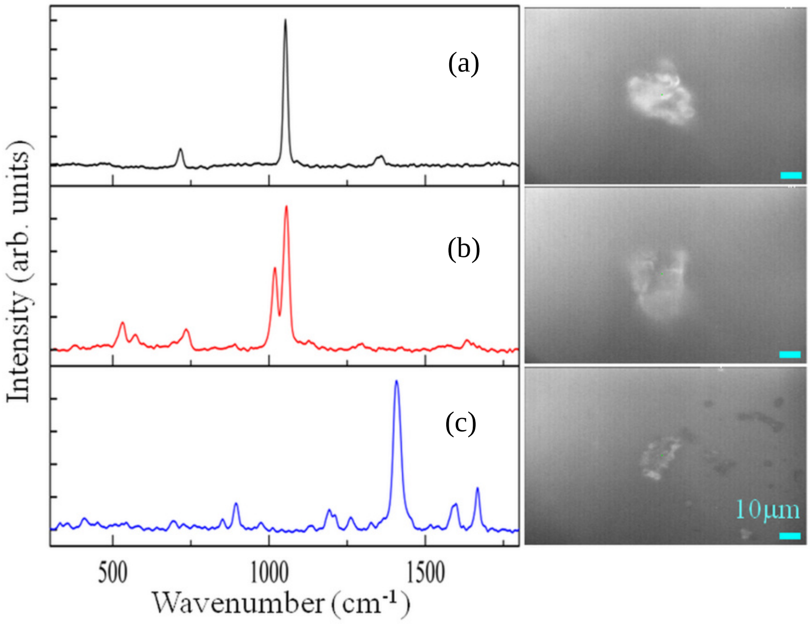

Fig. 8. Raman spectra of (a) potassium nitrate, (b) urea nitrate and (c). 2,4 dinitrotoluene. The image of the individual particles, obtained from the fingerprint residues of the different compounds, which were used for measuring the corresponding spectra.

To summarize, a modular, compact Raman spectrometer, based on a green laser pointer, was developed and applied for point detection of various materials. The feasibility of this setup for Raman spectroscopy of liquids in glass vials, trace amounts of explosives and even individual particles obtained from residues of latent human fingerprints with high sensitivity was demonstrated. Its point and real time detection capabilities for harmful compounds, together with the portability that it offers make it a potential candidate for field applications and open the door for future improvement by replacing the exciting source to a pulsed one in the Raman spectrometer and even more so by the outputs of the microchip laser + PCF for broadband

B-CARS, which is expected to lead to even higher sensitivities and even applicable for *standoff detection.*

References

---

[1] J. I. Steinfeld and J. Wormhoudt. Annu. Rev. Phys. Chem. **45**, 203 (1998).

[2] M. Nambayah and T. I. Quickenden, Talanta, **63**, 461 (2004).

[3] D. K. Williams, C. J. Brown and J. Bruker, Forensic Sci. Int. **206**, 161 (2011).

[4] E. R. Menzel, R. A. Bartsch and J. L. Hallman, J. Forensic Sci. **35**, 25 (1990).

[5] C. E. Allred and E. R. Menzel, Forensic Sci. Int. **85**, 83 (1997).

[6] Y. Mou and J. W. Rabalais, J. Forensic Sci. **54**, 846 (2009).

[7] J. Yinon. Trand. Anal. Chem. **21**, 292 (2002).

[8] J. C. Carter, S. M. Angel, M. Lawrence-Snyder, J. Scaffidi, R. E. Whipple and J. G. Reynold, Appl. Spec. **59**, 769, (2005).

[9] S. Wallin, A. Pettersson, H. Ostmark and A. Hobor, Anal. Bioanal. Chem. **395**, 259 (2009).

[10] D. S. Moore, Rev. Sci. Instrum. **75**, 2499 (2004).

[11] D. S. Moore, Sens. Imaging **8**, 9 (2007).

[12] J. Shu, I. Bar and S. Rosenwaks, Appl. Phys. B **70**, 621 (2000).

[13] J. Shu, I. Bar and S. Rosenwaks, Appl. Phys. B **71**, 665 (2000).

[14] O. Samek, D. C. S. Baddow, H. H. Telle, G. W. Morris, M. Liska and J. Kaiser, Appl. Phys. A **96**, 179 (1999).

[15] A. K. Rai, F. Y. Yueh and J. P. Singh, Appl. Opt. **42**, 2078 (2003).

[16] A. Portnov, S. Rosenwaks and I. Bar, Appl. Opt. **42**, 2835 (2003).

[17] M. Abdelhamid, F. J. Fortes, M. A. Harith and J. J. Laserna, J. Anal. Atom. Spectrom. **26**, 1445, (2011).

[18] D. Heflinger, T. Arusi-Parpar, Y. Ron, and R. Lavi, Opt. Comm. **204**, 327 (2002).

[19] M. K. K. Oo, C. F. Chang, Y. Sun and X. Fan, Analyst, **138**, 2811 (2011).

[20] K. J. Albert and D. R. Walt. Anal. Chem. **72**, 1947 (2000).

[21] D. L. Huestis, G. P. Smith, and H. Oser, Proc. SPIE-Int. Soc. Opt. Eng. **7679**, 76790G (2010).

[22] B. Zachhuber, G. Ramer, A. Horbo, E. t. H. Chrysostom and B. Lendl. Anal. Bioanal. Chem. **400**, 2439 (2011).

[23] M. D. Ray, A. J. Sedlacek and M. Wu, Rev. Sci. Instr. **71**, 3485 (2000).

[24] S. K. Sharma, A. K. Misra, P. G. Lucey, S. M. Angel and C. P. McKay, Appl. Spectrosc. **60**, 871 (2006).

[25] J. M. Hollas, *Modern Spectroscopy,* 3th Ed. John Wiley and Sons, Chichester (1997).

[26] S. K. Sharma, P. G. Luccy, M. Ghose, H. W. Hubble and K. A. Horton, Spectrochim. Acta A **59**,2391 (2003)

[27] D. S. Moore and R. J. Scharff, Anal. Bioanal. Chem. **393**, 1571 (2009).

[28]. H. Li, D. A. Harris, B. Xu, P. J. Wrzesinski, V. V. Lozovoy, and M. Dantus, Opt. Express **16**, 5499 (2008).

[29]. O. Katz, A. Natan, Y. Silberberg, and S. Rosenwaks, Appl. Phys. Lett. **92**,171116 (2008).

---

[30] D. A. Long, *The Raman Effect*. John Wiley and Sons, Chichester (2002).

[31] J. J. Valentini, Laser Spectroscopy and its Applications (Opt. Eng. Series, **11**), 507 (1987).

[32] A. Portnov, I. Bar, and S. Rosenwaks, Appl. Phys. B **98**, 529 (2010).

[33] N. Djaker, P. F. Lenne, D. Marguel, A. Colonna, C. Hadjur, H. Rigneault, Nucl. Instrum. Meth. A **571**,177 (2007).

[34] S. Yang, R. B. Wysolmerski and F. Ganikhanov, Opt. Lett. **36**, 3849 (2011).

[35] G.I. Petrov, R. Arora, V.V. Yakovlev, X. Wang, A.V. Sokolov and M. O. Scully, Proc. Natl. Acad. Sci. **104**, 7776 (2007).

[36] A. Zumbusch, G. R. Holton and X. S. Xie, Phys. Rev. Lett. 82, 4142 (1999).

[37] J. X. Cheng, Y. K. Jia, G. Zheng and X. S. Xie, Biophys. J. **83**, 502 (2002)

[38] G.I. Petrov, V.V. Yakovlev, A.V. Sokolov and M.O. Scully, Opt. Express **13**, 9537 (2005).

[39] A. Portnov, S. Rosenwaks and I. Bar, Appl. Phys. Lett. **93**, 041115 (2008).

[40] J. J. Zayhowski and C. Dill III, Opt. Lett. **19**, 1427 (1989).

[41] J. J. Zayhowski, Opt. Mat. **11**, 255 (1999).

[42] J. J. Zayhowski, J. Alloy. Compd. **303-304**, 393 (2000).

[43] G. I. Petrov and V. Yakovlev, Opt. Express **13**, 1299 (2005).

[44] J. M. Dudly, G. Genty and S. Coen, Rev. Mod. Phys. **78**, 1135 (2006).

[45] N. Djaker, D. Gachet, N. Sandeau, P. F. Lenne and H. Rigneault, Appl. Opt. **45**, 7005 (2006).